

Theoretical Study of Stubs for Power Line Noise Reduction

Toru Nakura, Makoto Ikeda*, and Kunihiro Asada*

Dept. of Electronic Engineering, *VLSI Design and Education Center (VDEC),
Univ. of Tokyo, Tokyo 113-8656, Japan
{nakura, ikeda, asada}@silicon.t.u-tokyo.ac.jp

Abstract— This paper describes a di/dt noise reduction method, which attaches stubs to the power line in LSI chips. A theoretical model of lossy transmission line stub is investigated, and simulation results show that the stub can reduce 48% and 26% of the noise compared with the nothing attached case, and de-coupling capacitor case, respectively, at a 2.5GHz 1.8V operation test circuit. It is also shown that this method will work more efficiently for further high frequency operation chips.

Introduction

While LSI chips generate more and more noise because of the high frequency operation and the increase of the transistor count on a chip, the low voltage operation decreases the noise margin. Thus, the power line noise is becoming a critical issue for reliability of the LSI functions. Since the operation frequency will get higher and higher in the future as the process technology proceeds, the di/dt noise caused by the high speed switchings and the inductances along the power lines will be a serious problem. EMI noise caused by di/dt is also becoming a critical issue.

In order to suppress the di/dt , some methods, such as a semi-asynchronous architecture[1] and an inserting de-coupling capacitor method[2] and using a complicated PCB board design[3] have been proposed. However, these methods make the circuit design complex and difficult, and an on-chip de-coupling capacitor requires more die area, an off-chip de-coupling capacitor doesn't work well due to the parasitic inductance on the terminal.

We propose a di/dt reduction method, which attaches stubs to the power lines in LSI chips. Stubs are widely used for impedance matching technique of wireline communications, where the loss of the transmission lines are ignored. Lossy transmission lines have been studied but only for signal wires[4]. This paper investigates an analytical model of lossy transmission line stubs suitable for the LSI noise reduction purpose. The HSPICE simulation results show that the stub suppresses about half of the di/dt noise.

Stub Theorem

A. Basics

As the operation frequency becomes higher and the wavelength of voltage and current gets comparatively smaller with the interconnect wire length, the wires should be considered as

transmission lines instead of lump RC elements. The characteristic impedance Z_0 , the propagation constant γ of the transmission lines are

$$Z_0 = \sqrt{\frac{R + j\omega L}{G + j\omega C}} \quad (1)$$

$$\gamma = \sqrt{(R + j\omega L)(G + j\omega C)} \quad (2)$$

where R, L, G, C are the resistance, inductance, admittance representing the dielectric loss, capacitance of the wire, per unit length respectively. The forward- and backward- going wave is expressed as $V_f e^{-\gamma z}$, $V_b e^{\gamma z}$. This expression can be transformed using phase constant β_r and attenuation constant α ,

$$V_f e^{-\gamma z} \equiv V_f e^{-\alpha z} e^{-j\beta_r z} = V_f e^{-(\alpha + j\beta_r)z} = V_f e^{-j(\beta_r - j\alpha)z}. \quad (3)$$

This equation leads that

$$\alpha = \text{real}(\gamma), \quad \beta_r = \text{imag}(\gamma) \quad (4)$$

and the complex phase constant β_c is defined as

$$\beta_c = \beta_r - j\alpha. \quad (5)$$

With using the complex phase constant, the forward- and backward- going wave are written as $V_r e^{-j\beta_c z}$ and $V_r e^{j\beta_c z}$, which are familiar expressions to us.

The input impedance of the transmission line with its characteristic impedance Z_0 , length l and termination impedance Z_l is

$$Z_{stub} = Z_0 \frac{Z_l \cos \beta_c l + j Z_0 \sin \beta_c l}{Z_0 \cos \beta_c l + j Z_l \sin \beta_c l}. \quad (6)$$

When open termination ($Z_l = \infty$),

$$Z_{stub} = Z_0 \frac{\cos \beta_c l}{j \sin \beta_c l}. \quad (7)$$

If the transmission line has no loss ($R = G = 0$) and its length is quarter of the signal wavelength ($\beta_c l = \pi/2$), the input impedance of the stub becomes zero ($Z_{stub} = 0$), which is equivalent with a infinite capacitance. When this stub is attached to the power line, the voltage fluctuation is suppressed.

The dominant frequency of the switching currents is the clock frequency f_0 . Thus, the stub length adjusted for the clock frequency becomes

$$l = \frac{\pi/2}{\beta_{r0}} = \frac{\lambda_0}{4} \quad (8)$$

where λ_0 is the signal wavelength in the transmission line. Once the stub length is decided for the frequency, the stub absorbs the noise at the frequency $(2n - 1)f_0$ as well, as known from eqn(7) since

$$\cos(\beta_c l) \approx \cos[(2n - 1)\beta_{r0}l] = \cos \frac{(2n - 1)\pi}{2} = 0. \quad (9)$$

Another stub, whose length is $l/2$, can also be attached for the second dominant frequency $2f_0$ and $(2n - 1) \cdot 2f_0$.

B. Equivalent Termination Approximation

Since the impedance of the power line itself is already small, the resistance of the stub is not negligible. The round trip attenuation factor η caused by the propagation loss in the lossy line is

$$\eta = e^{-\alpha 2l}. \quad (10)$$

The propagation loss is the only loss when lossy line with an open termination, while the reflection is the only loss when lossless (ideal) line with an finite termination impedance. Here, we propose a concept of equivalent termination impedance Z_{lEquiv} which induces a loss at the reflection Γ_{lEquiv} with the ideal line, as the same amount of the round trip propagation loss η with the lossy line, as shown in Fig.1.

$$\eta = \Gamma_{lEquiv} \equiv \frac{Z_{lEquiv} - Z_{0Ideal}}{Z_{lEquiv} + Z_{0Ideal}}. \quad (11)$$

From this equation, the equivalent impedance value becomes

$$Z_{lEquiv} = Z_{0Ideal} \frac{1 + \eta}{1 - \eta} = \sqrt{\frac{L}{C}} \cdot \frac{1 + \eta}{1 - \eta} \quad (12)$$

then, the input impedance of the quarter length stub ($\beta_r l = \pi/2$) becomes

$$Z_{stubEquiv} = Z_{0Ideal} \frac{Z_{lEquiv} \cos(\frac{\pi}{2}) + jZ_{0Ideal} \sin(\frac{\pi}{2})}{Z_{0Ideal} \cos(\frac{\pi}{2}) + jZ_{lEquiv} \sin(\frac{\pi}{2})} \quad (13)$$

$$= \frac{Z_{0Ideal}^2}{Z_{lEquiv}} = Z_{0Ideal} \frac{1 - \eta}{1 + \eta} = \sqrt{\frac{L}{C}} \cdot \frac{1 - \eta}{1 + \eta}. \quad (14)$$

Note that the Z_{lEquiv} and $Z_{stubEquiv}$ are frequency independent once the stub length is decided.

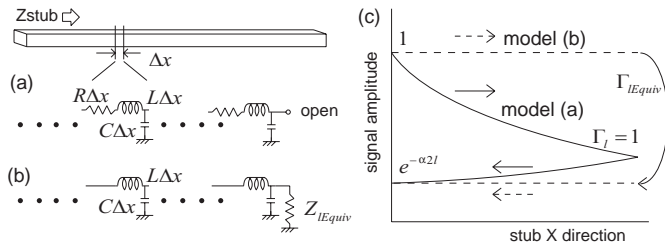


Fig. 1. (a). Lossy transmission line with an open termination — realistic model, (b). Lossless transmission line with the equivalent termination impedance — equivalent termination approximation, (c). The signal amplitude distribution along the stub.

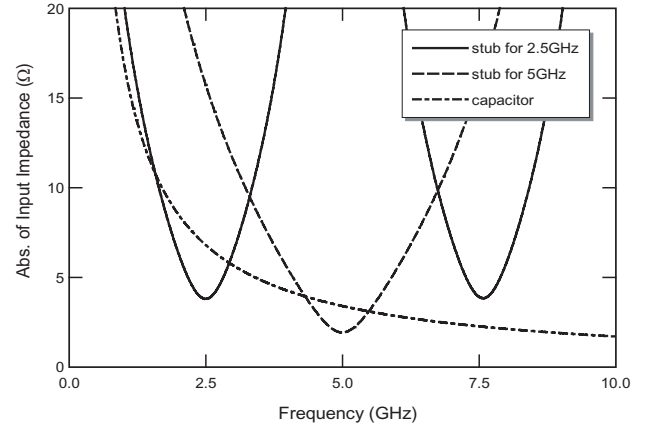


Fig. 2. Frequency dependence of the input impedance of the stub and the capacitor.

C. Stub Optimization

If a wider stub width is used in order to reduce the resistance of the stub and the input impedance, the de-coupling capacitance fabricated with the same space becomes bigger so that the noise reduction of the stub and of the de-coupling capacitor cannot be distinguished. Since the purpose of this study is to estimate the noise reduction effects of stubs, the stub structure was decided so as to maximize the noise difference between the stub and the de-coupling capacitor. Of course, wider stubs are more efficient from noise reduction point of view, if there is no space limitation.

We assumed a $0.18\mu\text{m}$ 5 metal CMOS process, in which 15.323mm and 7.662mm length of $40\mu\text{m}$ width stub using ML4, ML5 together with ML1 Gnd plane is the optimized condition for a 2.5GHz operation circuit to observe the noise difference. The transmission line parameters of this structure is $R=500\Omega/\text{m}$, $L=102\text{nH}/\text{m}$, $C=407\text{pF}/\text{m}$, according to the 2-D Raphael simulation, and no dielectric loss ($G=0$) is assumed here. The de-coupling capacitance of the same space is $C_p = 407\text{pF}/\text{m} \times (15.323 + 7.662\text{mm}) = 9.4\text{pF}$. The frequency dependence of the input impedance of the stub from eqn(7) and of the capacitor $|Z_{cap}| = 1/\omega C_p$ with this structure are shown in Fig.2. The stub input impedance is smaller than the capacitor input impedance at the designed frequency.

Here, we assumed that the current density is constant inside the stub, without considering the skin effects.

Simulation

A. Test Circuit

Fig.3 shows our test circuit, which is a PRBS (Pseudo Random Bit Stream) $2^7 - 1$ generation circuit with some inverters at each port. The number of the inverters is distributed from 2 to 12, which represents a path length distribution between DFFs in common synchronous circuits. The delay of the longest inverter chain is smaller than 2.5GHz clock period. We tested three kinds of the power line as the reference: nothing attached, the same space de-coupling capacitor, and the stub. The inductance of the bonding wire and the lead frame is assumed to be 0.5nH .

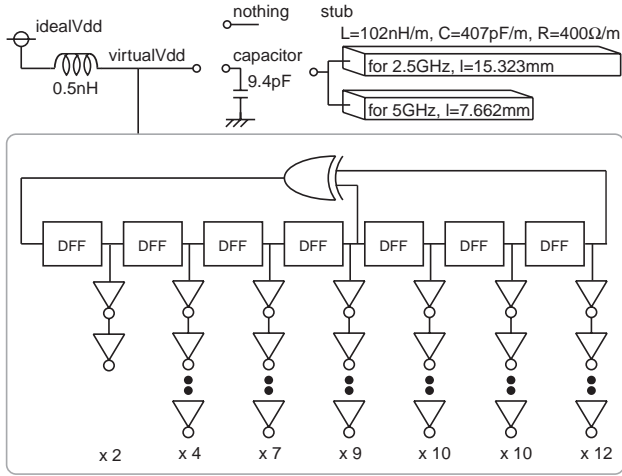


Fig. 3. Test circuit

B. Simulation Technique

The stub can be modeled as a RLC ladder as shown in Fig.1(a) for SPICE simulations. However, the number of the ladder step have to be big in order to suppress the LC resonant ringing which doesn't occur in reality. Also, the inductors make simulation convergence difficult and take longer simulation time. By the equivalent termination approximation using an ideal transmission line element and the equivalent termination impedance as eqn(12), the simulation time decreased 13% in our test case.

C. Simulation Results

Fig.4(a) shows the HSPICE simulation waveforms of the virtualVdd node in Fig.3 with the three power line structures, and (b) shows the corresponding spectrum, at 1.8V 2.5GHz operation. The standard deviation σ from the ideal Vdd value are 0.107/0.075/0.055 for the nothing/capacitor/stub case respectively. This means the stub suppressed 48%/26% of the noise compared with nothing/capacitor case. Also, the stub suppressed 58%/36% of the 2.5GHz noise component, and 63%/36% of the 5GHz noise component, compared with the nothing/capacitor case, respectively.

Discussion

A. Frequency Components

If switching timing of transistors is always the same at every clock cycle, the current contains only nf_0 components. However, the random switchings at each clock cycle in LSI cause non- nf_0 component which the stubs cannot absorb, as shown in Fig.4(b).

The input impedance of the stub is Z_0 at the initial condition, and Z_{stub} at the steady state. It needs time constant τ to change the input impedance from Z_0 to Z_{stub} . The time constant is expressed as

$$\tau = \frac{1}{-2f \log |\eta \Gamma_s|} \quad (15)$$

where Γ_s is the reflection coefficient at the near end. The time constant is 557ps/603ps for 2.5GHz/5GHz stubs, which are

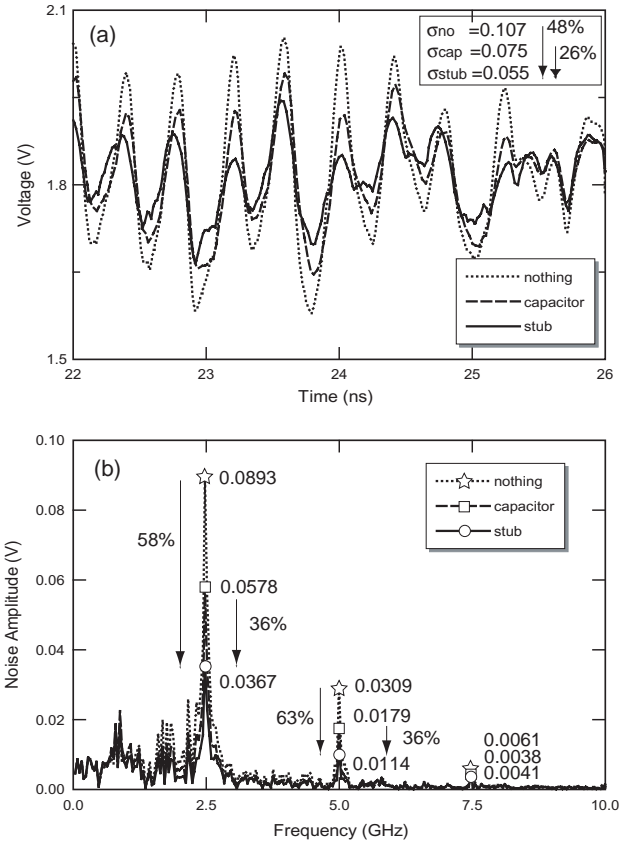


Fig. 4. (a). Simulated waveforms of the virtualVdd node, and (b). corresponding spectrum.

less than two clock cycles in our test case.

The non- nf_0 components and the time constant disturb the noise reduction effect of the stub. But still, the stub can suppress some amount of the power line noise, as shown in Fig.4(a).

B. Voltage Swing at the End Terminal

The stub suppresses the noise because it stores and provides the energy of the specified frequency so that the AC current doesn't go through the bonding wire inductance. The energy is stored by swinging the signal in the stub, and the far end terminal has the maximum amplitude of the voltage. The ratio of the voltage at the near end and the far end is

$$\frac{V_{far}}{V_{near}} = -j \frac{1 + \eta}{1 - \eta} \quad (16)$$

at the steady state, if the equivalent termination approximation is used. The ratio is 4.26, 8.27 for 2.5GHz, 5GHz stubs in our test case. When the stub is used in a LSI, the attention should be paid so as not to exceed the break down voltage of the insulator between the metal layers, since the voltage at the end terminal becomes higher than the supply voltage.

Fig.5(a) shows the waveforms of the near and the far end of the stub modeled by the equivalent termination approximation, and modeled by the 100 stage LCR ladder. The equivalent termination approximation agrees with the 100 stage LCR ladder. The spectrum of the far end of the 2.5GHz and 5GHz

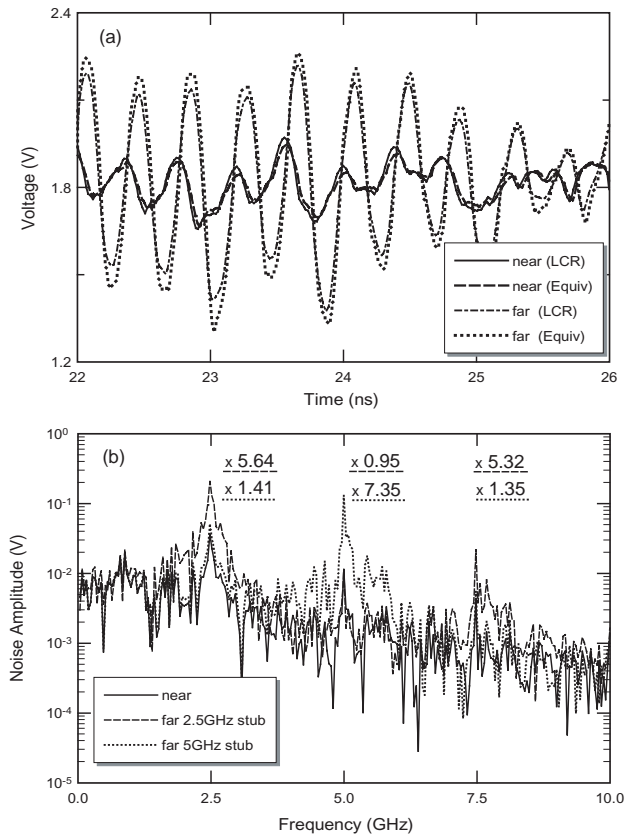


Fig. 5. (a). Waveforms of the near end (virtualVdd) and the far end of the 2.5GHz stub. 100 stage LCR ladder, and the equivalent termination approximation case. (b). The corresponding spectrum of the far end of the 2.5GHz and 5GHz stub, and the near end, with the equivalent termination approximation case.

stub, and the near end, with the equivalent termination approximation case are shown in Fig.5(b). This graph shows that the 2.5GHz stub stores the energy around 2.5GHz and 7.5GHz components, and the 5GHz stub for 5GHz component, which agree with the frequency dependence of the stub calculated in Fig.2. The ratio value difference from eqn(16) is because this is a transient simulation result, not a steady state analysis.

C. Higher Frequency Case

The stub length, thus the de-coupling capacitance value as well, are in inverse proportion to the operating frequency. Then the input impedance of the capacitor $|Z_{cap}|=1/\omega C_p$ is constant to the frequency, while the input impedance of the stub gets smaller since the shorter stub length reduces the effects of the resistance. Fig.6 shows the operation frequency dependence of the input impedance of the stub and of the corresponding de-coupling capacitor, with the same stub structure as the test case. The input impedance reduction ratio at the Chip Frequency in the ITRS road map[5] with the corresponding year are also shown.

Since the noise amplitude is decided by the parasitic inductance, vdd-gnd capacitance, source-well capacitance and so on as well as the stub input impedance, the input impedance reduction ratio is not equal to the noise reduction ratio. However, a stub with a smaller input impedance can suppress more

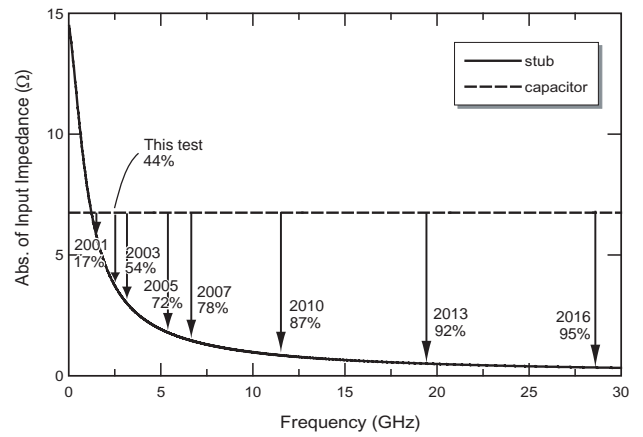


Fig. 6. Operating frequency dependence of the input impedance of the stub and the de-coupling capacitor. The input impedance ratio at the Chip Frequency in the ITRS road map with the corresponding year are also shown.

noise, and we can see that the stub will work more efficiently for the noise reduction in the near future as the clock frequency advances.

Conclusion

The stubs for power line noise reduction have been demonstrated. The analytical model of the lossy transmission line stubs suitable for the LSI power line noise reduction purpose was investigated. Circuit simulation results showed that the stub reduces 48% and 26% of the di/dt noise compared with the nothing attached case, and de-coupling capacitor case, respectively, in our 1.8V 2.5GHz test circuit. Furthermore, the stub can suppress the noise more efficiently in higher speed LSIs, which will hit our technology trend.

References

- [1] Mustafa Badaroglu, Kris Tiri, Stephane Donnay, Piet Wambacq, Ingrid Verbauwhede, Georges Gielen, Hugo De Man, "Clock Tree Optimization in Synchronous CMOS Digital Circuits for Substrate Noise Reduction Using Folding of Supply Current Transients," in *Proc. 39th Design Automation Conf.*, June 2002, pp.399-404.
- [2] K. Y. Chen, William D. Brown, Leonard W. Schaper, Simon S. Ang, Hameed A. Naseem, "A Study of the High Frequency Performance of Thin Film Capacitors for Electronic Packaging," *IEEE Trans. Advanced Packag.*, May 2000, pp.293-302.
- [3] Hirokazu Tohya, "New Technologies Doing Much for Solving the EMC Problem in the High Performance Digital PCBs and Equipment," *IEICE Trans. Fundamentals*, March 1999, pp.450-456.
- [4] Payam Heydari, Soroush Abbaspour, Massoud Pedram, "A Comprehensive Study of Energy Dissipation in Lossy Transmission Lines Driven by CMOS Inverters," in *Proc. 2002 Custom Integrated Circuits Conf.*, May 2002, 25-6.
- [5] "International Technology Roadmap for Semiconductors 2002 Update," [Online] Available: <http://public.itrs.net/>